Inertial Density Currents over Porous Media Limited by Different Lower Boundary Conditions

L. P. Thomas[1] and B. M. Marino[2]

Abstract: We study the evolution of two-dimensional high-Reynolds-number density currents propagating over horizontal porous substrates initially saturated with a lighter fluid when an impermeable surface under the bed is used and a Darcy flow through the medium takes place. Laboratory experiments were performed varying the initial characteristic parameters such as the volume released, the height-to-width ratio of the dense fluid, the relative density difference between the current and ambient fluids, and the bed depth. The dynamic changes of the gravity-driven flow and the influence of the thickness of the porous substrate are described by means of an empirical analysis that considers two lower boundary conditions of the bed, that is, when it is bounded from below by an impermeable or a permeable layer. Thus, the new experimental results are integrated to previous findings in a unified theoretical treatment. In the present case, the dense fluid penetrates into the porous layer pushing the lighter one through the upper boundary located ahead of the current, as shown by the vorticity distribution, and modifying the interaction between the flows over and inside the bed. This flow in the neighborhood of the front, although important, is smaller than the one that would pass through the lower boundary if this were permeable. **DOI: 10.1061/(ASCE)HY.1943-7900.0000477.**

CE Database subject headings: Density currents; Porous media; Stratified flow; Measurement.

Author keywords: Density currents; Porous media; Stratified flow; Laboratory measurements.

Introduction

Gravity, density, or buoyancy currents are flows driven by a density difference between the current and the ambient fluid into which it penetrates. Many of them are of considerable scientific and practical importance to environmental sciences, geophysics, chemical and hydraulic engineering, and oceanography as the comprehensive review by Simpson (1997) shows. The wide range of situations in which these flows appear has motivated a great number of basic and applied research. We will consider the propagation of gravity currents over horizontal porous layers initially saturated with an ambient fluid. As the current fluid sinks into the bed driven by the excess pressure at the top of the layer, the loss of mass through the porous medium reduces the driving force of the current and thereby affects its velocity and thickness. This kind of flow occurs frequently in varied natural situations that include the currents of brackish water generated by tidal motions over the permeable bottom of estuaries, internal waves impinging on continental shelves, and the irrigation waters that wander naturally to aquifers through a porous substrate. In addition, man-made situations involve the release of sewage liquids on nearby coasts and the accidental escape of toxic liquids from containers surrounded by gravel beds or a thick vegetal cover, among others. An important application is in the petroleum industry, where crude oil is trapped in natural underground reservoirs that consist of porous sedimentary formations such as sand, stone, limestone, and dolomite usually disposed in layers of different permeability. The most important practical aspect related to the dynamics of the flows over and within the porous medium is the determination of the mass absorbed by the bed and the maximum distance the current travels before stopping. Knowledge of this length and the determination of the stage in which the dilution of the fluid in the adjacent environment decreases below a threshold value would be very useful for safety calculations concerning, e.g., pollutants dispersion.

There are many studies of flows in steady-state over a porous medium. Prinos et al. (2003) reviewed the main works related to the effect of a porous bed on the free flow above it and the flow characteristics near the interface for laminar and turbulent cases, and described a few applications of the hydrodynamic effects of the interface on water quality and mass transfer. They presented a computational study of the turbulent flow features in a two-dimensional open channel with a permeable bed simulated by different arrangements of cylindrical rod bundles placed perpendicular to the flow and compared the results with experimental findings. In addition to this problem, research of the non-steady-state of flows such as gravity currents propagating over porous media have been addressed both theoretically and experimentally. For currents flowing over thin porous substrates, only the weight of the overlying fluid drives drainage (Thomas et al. 1998; Ungarish and Huppert 2000; Pritchard et al. 2001; Marino and Thomas 2002). Previous experimental works related with inertial gravity currents (that is, with Reynolds number $R \gg 1$) were first devoted to study the release of saltwater flows over horizontal porous surfaces modeled by metallic grids inside a rectangular cross section tank filled with tap water, considering viscous (Thomas et al. 1998) and inertial (Marino and Thomas 2002) flows through the substrate. For a viscous flow inside a bed of thickness ε with Reynolds number of the flow through the porous medium $R_{PM} \leq 1$, Darcy's law

[1]Professor, Facultad de Ciencias Exactas, Universidad Nacional del Centro de la Provincia de Buenos Aires, Pinto 399, B 7000 GHG Tandil, Argentina (corresponding author). E-mail: lthomas@exa.unicen.edu.ar

[2]Professor, Facultad de Ciencias Exactas, Universidad Nacional del Centro de la Provincia de Buenos Aires, Pinto 399, B 7000 GHG Tandil, Argentina.

Note. This manuscript was submitted on November 15, 2010; approved on June 21, 2011; published online on June 23, 2011. Discussion period open until July 1, 2012; separate discussions must be submitted for individual papers. This paper is part of the ***Journal of Hydraulic Engineering***, Vol. 138, No. 2, February 1, 2012. ©ASCE, ISSN 0733-9429/2012/2-133–142/$25.00.

(Bear 1972) is valid and, as found, gravity currents lose mass at an exponential rate through the porous surface with a constant of decay $\tau_D = \nu\varepsilon/\kappa g_0'$ where g_0' = initial reduced gravity, ν = kinematic viscosity of the fluid, and κ = permeability of the bed, while the front velocity and the current height also decrease exponentially. The loss of mass dominates the flow and, in contrast to gravity currents evolving over solid bottoms, no self-similar regime is developed. In the case of an inertial flow (that is, $\mathrm{R_{PM}} > 1$) through a layer of high permeability and small thickness, the mass of the gravity current also decreases exponentially but with a different constant of decay $\tau_I = \beta A_0^{1/4} g_0'^{-1/2}$ where β = constant and A_0 = initial lateral area of the fluid released.

In contrast, for gravity currents propagating over deep porous media, Acton et al. (2001) showed that both the hydrostatic pressure of the fluid in the current and the weight of the fluid within the porous medium drive drainage. They used this description of drainage in a model of experiments in which low-Reynolds-number gravity currents spread over a deep porous layer consisting of small glass spheres. Thomas et al. (2004) analytically and experimentally investigated plane high-Reynolds-number gravity currents traveling over a thick porous bed, confirming that the fluid mass lost from the current through the bed is well described by Darcy's law and scales on the timescale τ_D mentioned above. They used an experimental setup in which there is a water channel below the porous bed and presented an integral model that describes the flow of the current in terms of a global mass balance suggesting an analytical approximation for extended currents. Such a solution provides a finite time of extinction in which all the mass of the current is lost. Pritchard and Hogg (2002) have also applied the same drainage law to their examination of gravity currents propagating within a porous medium overlying a deep layer of lower permeability.

Numerical models concerning the study of releases of fixed volumes of liquids under the shallow water approximation including the cases of downward porous slopes (Moodie and Pascal 1999b) and with axial symmetry (Moodie and Pascal 1999a) were also reported. Ungarish and Huppert (2000) studied analytically and numerically the consequences in the evolution of the flow because of the presence of an impermeable bottom of the lock where the dense fluid is initially contained in the experimental setup used by Thomas et al. (1998). They argued that the gravity flow evolution depends on the decay constant τ_D but also on the characteristic time $t_c = x_0/\sqrt{g_0' h_0}$ related to the initial height h_0 and length x_0 of the lock where the dense fluid remains before release for $t \approx t_c$. More recently, Spannuth et al. (2009) studied the axisymmetric propagation of a viscous gravity current over a deep porous medium for the fixed-flux case and presented a model that uses lubrication theory for flow within the current, the drainage law of Acton et al. (2001), and Darcy flow within the porous medium. While the full spatial and temporal evolution of the current can only be obtained numerically, an analytical expression for the steady-state extent and profile of the current is found. Additionally, they developed scaling laws describing the propagation of the current.

As that by Thomas et al. (2004), this paper is also concerned with the releases of fixed volumes of a dense fluid that propagates under the influence of gravity inside a lighter miscible fluid and over a horizontal permeable substrate. Now, as the schematic diagram in Fig. 1(a) depicts, a solid base limits the porous medium causing a different flow inside it that is relevant to the gravity current evolution. We describe the results of new laboratory experiments in which the influence of the initial reduced gravity, the thickness of the substrate and the volume of dense fluid released is explored. After that, an analytical model is provided to describe the influence of this lower boundary condition on the flows over and through the permeable bed, which includes the case sketched in Fig. 1(b). The latter may be now considered as a particular case of the flow through a thick porous medium where Darcy's law is valid. Thus, the main contribution of this paper is not only to present the results found using a new experimental configuration and support them theoretically, but also to integrate them to previous findings into a unified framework in order to understand the effect of the flow inside the bed on gravity currents and its relative importance on the dynamics of the global situation. Finally, the concluding remarks are given.

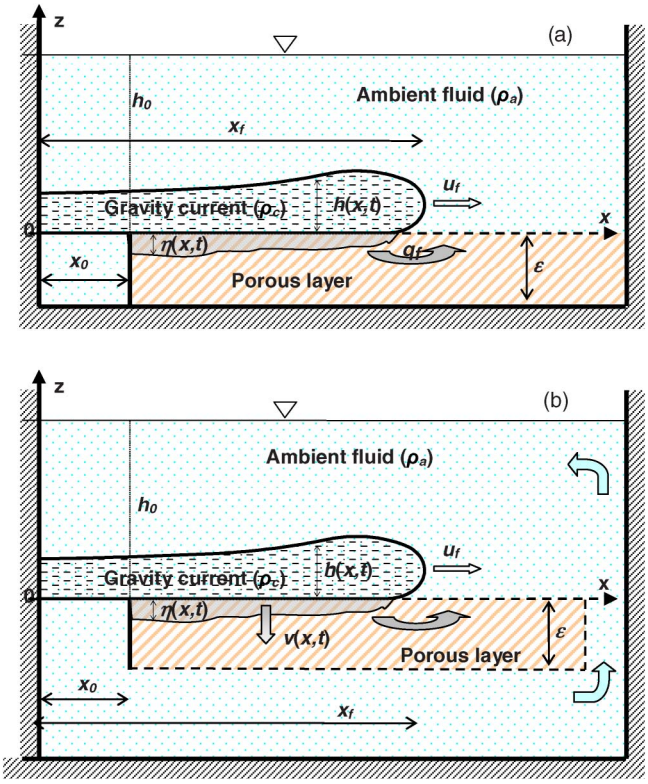

Fig. 1. Schematic views of gravity current above porous bed saturated with ambient fluid; porous medium is bounded by: (a) impermeable surface as in this study; (b) permeable layer as in situation considered by Thomas et al. (2004)

Experimental Procedure

Laboratory experiments were carried out by releasing fixed volumes of salt water, colored to provide visualization, from behind a lock with impermeable base into a rectangular cross section channel (3.0 m long, 0.2 m wide, and 0.6 m deep, with transparent Perspex sidewalls) containing fresh water up to a depth h_0 above the porous bottom. A vertical barrier located at a distance x_0 from the rear wall is suddenly removed at $t = 0$, allowing the dense fluid to flow out along the porous bed. The porous medium, of porosity $\varphi = 0.375$ and permeability $\kappa = 6 \times 10^{-5}$ cm^2, is composed of small glass spheres of 0.00286 m average diameter and saturated with fresh water. After each run, the porous layer was washed with fresh water and dried with warm air in order to avoid the formation of random bubbles inside that might affect the reproducibility of the results. The influence of the porous bed on the gravity currents was investigated varying the lateral area $A_0 = x_0 h_0$ of the initial released volume of the dense fluid, the density relative difference $\Delta\rho/\rho$, and the thickness ε of the bed. The evolution of the front position, maximum height, and mass of the current is also determined.

The dense fluid mass per unit width over the porous medium is obtained applying image processing. Behind the channel, a panel of lights with a diffusing screen provided uniform backlighting. The images captured by a COHU 4910 video camera placed at a fixed position 6 m away from the tank were stored online and digitally processed later. As the region of practical interest is approximately 3 m long and 0.30 m height, an anamorphic lens system is used to enlarge the vertical scale and reduce the horizontal by a factor 2. Measurements of the light intensity related to the concentration of the dye along each light path are obtained for each pixel, so providing the width averaged dye concentration. Because the dye acts as a passive tracer, its concentration is associated with the width averaged salt concentration. Thus, the intensity measurements give the two-dimensional density distribution $\rho(x,z,t)$-ρ_a on each video frame, and the current mass m per unit width is obtained by integrating this density distribution. The error of m is found to be less than 2% by calculating the mass of a dense current evolving over an impermeable bottom at different times. As it is constant independently of the mixing between current and ambient fluids, the deviation of the measured values from the initial one gives an estimate of the error of the whole image processing. More details of the calibration procedure can be found in the work by Hacker et al. (1996). Because of the opacity of the glass spheres, it was only possible to obtain density measurements above the porous layer.

Particle image velocimetry (PIV) was also applied to find the velocity and vorticity fields around the current front. Particles of Pliolite VT (a granular resin used in the manufacture of solvent-based paints) of density 1.02 g/cm^3, similar to the fluids, were sieved to obtain sizes in the range 300–500 μm and added to dense and ambient fluids. The experiment was illuminated by a 500 W halogen lamp with a linear filament that was focused by a lens into a vertical light sheet, approximately 0.01 m thick, entering through a slot made in a Perspex sheet located on the water free surface and cutting along the central part of the tank. The use of this Perspex sheet avoids the light intensity variations produced by the motion of the free surface liquid. After completing an experiment, the images captured were digitally processed employing the software DigiFlow (Dalziel 2006) to determine the instantaneous velocity gradient field that is used to obtain the vorticity distribution.

Laboratory Results

Table 1 introduces the main parameters of the runs performed while Fig. 2 shows the gravity current as seen in a typical experiment under the boundary conditions of our interest. The images are in a color scale that is related to the fluid density and show a number of features, some of which are observed in currents over an impermeable base while others result from the penetration into the bed. Initially, the flow is essentially the same as over a solid bottom: the density in the bulk does not change during the collapse, a sharp horizontal density gradient marks the current front, and the characteristic head, deeper than the following current, forms. The dense fluid moves horizontally while billows appear on the top. As the current evolves, its depth (at any given horizontal location) and the density (mainly in the head) decrease, as the variation in color evidences. In general, it is observed that the changes resulting from the penetration of dense fluid into the porous bed depend on the relative density difference.

Quantitatively the dynamics of the gravity current leading part for all the experiments performed is not strongly affected by the reduction of the global mass during the time that a run lasts. Fig. 3 illustrates the classical evolution of the front position of gravity currents for three different porous layer thicknesses. The same

Table 1. Main Parameters for Set of Laboratory Experiments

Run	$\Delta\rho/\rho$	ε	x_0	h_0	R
1	0.0049	0	0.152	0.300	12,700
2	0.0097	0	0.153	0.300	18,000
3	0.0115	0	0.199	0.300	19,500
4	0.0115	0	0.298	0.200	10,600
5	0.0170	0	0.152	0.300	23,800
6	0.0370	0	0.151	0.300	35,000
7	0.0058	0.03	0.151	0.301	13,900
8	0.0107	0.03	0.152	0.200	10,300
9	0.0107	0.03	0.149	0.150	6,600
10	0.0107	0.03	0.201	0.200	10,300
11	0.0108	0.03	0.151	0.301	19,000
12	0.0210	0.03	0.152	0.300	26,400
13	0.0403	0.03	0.152	0.299	36,300
14	0.0058	0.09	0.167	0.309	14,500
15	0.0107	0.09	0.151	0.307	19,500
16	0.0107	0.09	0.148	0.210	11,000
17	0.0107	0.09	0.147	0.156	7,100
18	0.0107	0.09	0.198	0.206	10,700
19	0.0108	0.09	0.153	0.400	29,100
20	0.0206	0.09	0.151	0.314	28,000
21	0.0409	0.09	0.146	0.315	39,700
22	0.0059	0.15	0.170	0.315	15,000
23	0.0109	0.15	0.166	0.327	21,600
24	0.0208	0.15	0.148	0.309	27,400
25	0.0404	0.15	0.161	0.325	41,100

Note: Initial values of Reynolds numbers are estimated using $\mathrm{R} = (h_0/2)(\sqrt{g' h_0/2})/\nu$.

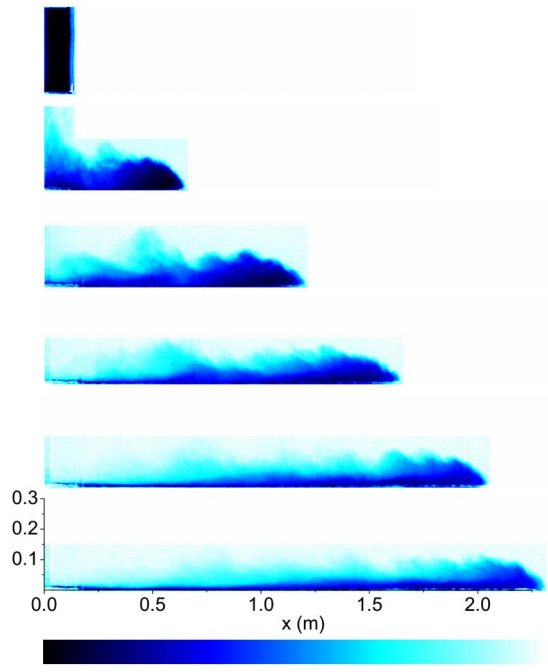

Fig. 2. False color-representation of gravity current evolving over porous layer ($\varepsilon = 0.03$ m) with an impermeable base for $\Delta\rho/\rho = 1\%$ at times $t = 0$, 8.04, 12.72, 19.14, 25.94 and 33.58 s from release; density scale is shown at bottom of figure

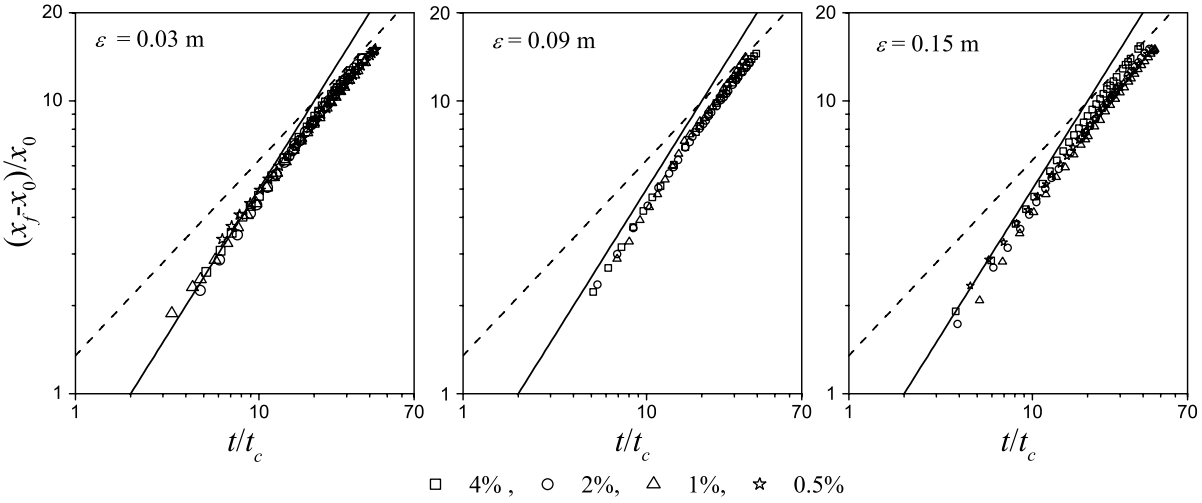

Fig. 3. Front position evolution of gravity currents for different ε and $\Delta\rho/\rho$

self-similar laws describing the slumping (solid lines) and inertial (dashed lines) current behavior over rigid bottoms are mostly valid to describe the front position evolution in the present configurations. Also, the same characteristic time t_c, based on the horizontal length x_0 and the initial velocity $\sqrt{g_0' h_0}$, results useful to provide a time dimensionless parameter in order to the experimental points corresponding to different bed thicknesses collapse onto single curves. However, a slight departure of this trend appears and more noticeably for the $\varepsilon = 0.09$ and 0.15 m cases at the latest times, even for experiments with the same x_0 and h_0 as shown in Fig. 3.

Hence, we must pay attention to the evolution of another more sensitive variable to visualize the effects of the porous bed on the current dynamics. Fig. 4 shows the variation of the dimensionless current mass $M(t)$, defined as the ratio between the dense fluid mass per unit width at time t located above the porous bed and the total saltwater mass per unit width released, for different initial density relative difference and porous medium thickness. The loss of mass for $\varepsilon = 0.03$ m (circles) is too small under the present experimental conditions and the results for $M(t)$, associated with the current lateral area $A(t)$, seem to coincide with those of the currents running over impermeable bottoms (squares). On the contrary, the decreasing of mass for $\varepsilon = 0.09$ (up-triangles) and 0.15 m (down-triangles) is noticeable, but significant differences between the results of both cases are not detected. For a given thickness, the greater the relative difference of density, the greater the loss of mass. In order to make this observation clear, we choose to represent M for the runs performed over a 0.15 m wide porous medium in Fig. 5 together with the curves provided by the analysis introduced in the section " Analysis of the Flows Involved." For small values of $\Delta\rho/\rho$, the mass variations detected are of the order of the experimental error but are clearly observed for $\Delta\rho/\rho \approx 2$ and 4%.

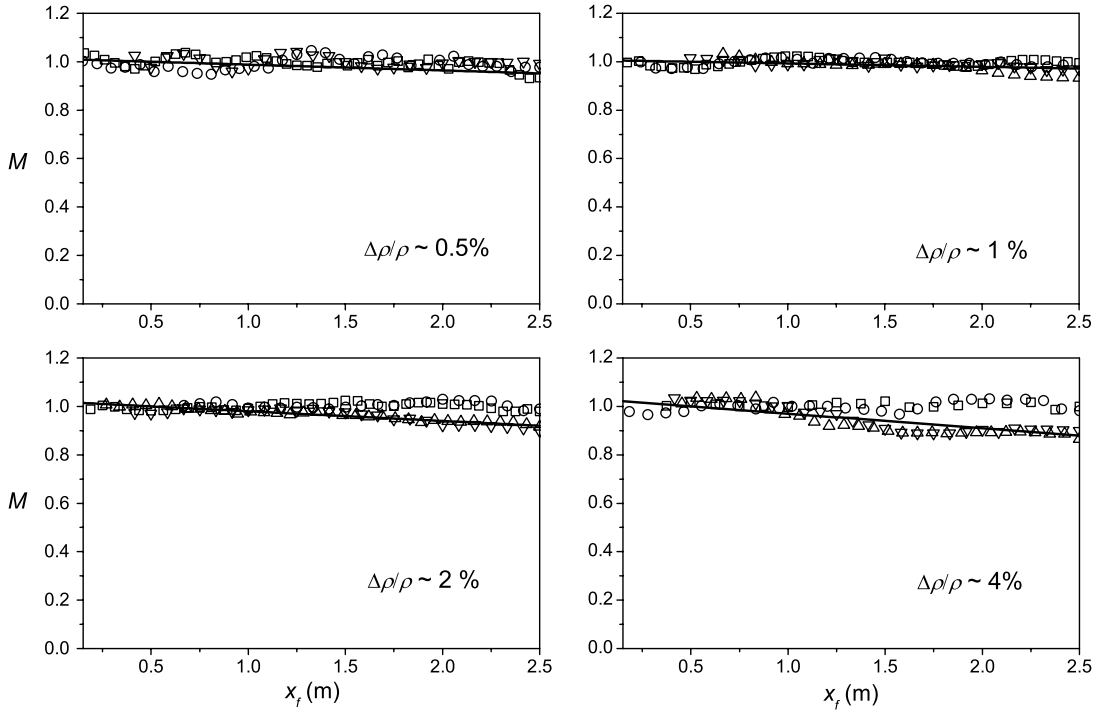

Fig. 4. Dimensionless current mass that remains over porous substrate for different ε and $\Delta\rho/\rho$

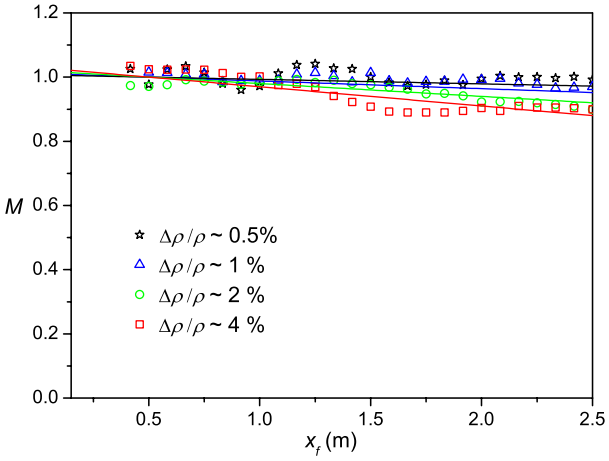

Fig. 5. Dimensionless current mass evolution for porous layer of thickness $\varepsilon = 0.15$ m and different $\Delta\rho/\rho$

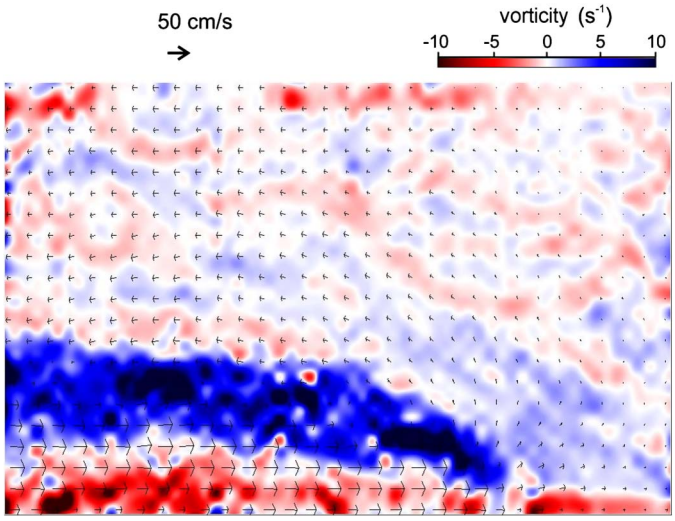

Fig. 6. Instantaneous distributions of velocity (arrows) and vorticity (false color) for gravity current evolving over 0.03-m deep porous substrate

On the other hand, it is interesting to observe Fig. 6, which shows the velocity and vorticity instantaneous distributions obtained by applying PIV technique around the frontal zone of a gravity current evolving over the porous bed. The circle marks the zone ahead of the current front that is influenced by the ambient fluid flow displaced from the bed because of the entrainment of dense fluid into it. The comparison with the case of a gravity current running over a rigid surface (Thomas et al. 2003) indicates that the vorticity is greater at the top of the current and that localized zones of negative vorticity appear near the interface dense fluid-porous bed. The roughness of this interface plays a significant role in the generation of vortices and turbulence within the gravity flow, probably implying a different erosive power in natural currents. This feature is analyzed by means of a separate series of experiments and the results are reported in a parallel work (Marino and Thomas 2010).

Analysis of Flows Involved

As shown in Fig. 1, after release, a gravity current of dense fluid (e.g., salt water) develops on the upper boundary of the porous layer at $z = 0$ while part of it flows into the bed. We assume that the transversal coordinate y plays no role and all the flow may be considered to be two-dimensional. The bed is saturated with a homogeneous ambient fluid that is displaced as the dense fluid sinks into it. Laboratory results show the current mass diminishes slowly as function of the front position along the extent of the present experimental setup (Figs. 4 and 5). The Reynolds number of the density-driven flow over the bed is sufficiently large to neglect the viscous forces and then a balance between buoyancy and inertial forces dominates the flow dynamics. The porous medium is homogeneous and isotropic on a macroscopic scale so that all the physical properties like porosity and permeability, are uniform. Although the flow through the porous layer involves dense fluid over lighter fluid, which makes it unstable, the convective instabilities are ignored for the purposes of this discussion.

Flow inside Porous Substrate

At the time when the gravity current front is at the position x_f, the hydrostatic pressure excess above the porous medium is

$$p(x, z=0) = \begin{Bmatrix} p_1(x) = \rho_a g' h & \text{for } x \le x_f \\ p_2 = 0 & \text{for } x > x_f \end{Bmatrix} \tag{1}$$

where ρ_c and ρ_a = densities of the current and surrounding fluids, respectively, and $g' = g(\rho_c - \rho_a)/\rho_a$ = reduced gravity with g = gravitational acceleration. Because of mixing between the fluids, ρ_c decreases while the current height h increases maintaining the value of the total buoyancy $\rho_a g' h$ at any given position x; therefore, the effects of mixing may be neglected at first approximation, ρ_c is assumed constant and the lateral area A of the current is proportional to its mass M.

The pressure at $z = -\varepsilon$ is determined by the fact that the normal velocity is zero on a solid impermeable surface as in Fig. 1(a) case, or by the hydrostatic pressure if it were permeable as in the situation represented in Fig. 1(b). The boundary condition at the interface between a porous medium and a solid surface has been studied by Haber and Mauri (1983), among others, and for the present investigation it may be obtained as follows. Within the porous medium, the flow per unit area is given by Darcy's law:

$$\bar{q} = -\frac{\kappa}{\mu}[\bar{\nabla} p - (\rho - \rho_a)\bar{g}], \tag{2}$$

where μ and ρ = dynamic viscosity and density of the fluid, respectively. At the lower impermeable boundary, it results

$$\frac{\partial p}{\partial z} = -(\rho - \rho_a) g \approx 0$$

because there is no flow when $\rho \approx \rho_a$. Therefore, by neglecting the effects of the impermeable bottom of the lock where the dense fluid is initially contained, the lower boundary condition for the porous layer is

$$\begin{Bmatrix} \frac{\partial p}{\partial z} = 0 & \text{for an impermeable boundary [Fig. 1(a)]} \\ p = 0 & \text{for a permeable boundary [Fig. 1(b)]} \end{Bmatrix} \tag{3}$$

in $z = -\varepsilon$ for $0 \le x \le x_m$, and moreover in $x = 0$ and $x = x_m \gg x_f$ for $-\varepsilon \le z \le 0$, where x_m = position far enough from the current front where the flow inside the bed is negligible.

Because the fluid in the pores is incompressible, it follows from (2) that

$$\nabla \bar{q} = \nabla^2 p - \bar{g} \cdot \bar{\nabla} \rho = 0. \tag{4}$$

The dense fluid gets into the porous layer for $x \le x_f$ causing the lighter fluid to go out through the upper boundary located at $x > x_f$ but also through the lower boundary at $z = -\varepsilon$ if it is permeable.

In Boussinesq's approximation, there are no significant differences between the fluid's densities (that is $\rho_c \approx \rho_a$), so that the flow inside the porous medium may be considered as the flow of a single homogeneous fluid at first approximation. This hypothesis is valid if

$$\nabla^2 p \gg \bar{g} \cdot \bar{\nabla} \rho = 0 \tag{5}$$

Therefore, Eq. (4) becomes

$$\nabla^2 p = \frac{\partial^2 p}{\partial x^2} + \frac{\partial^2 p}{\partial z^2} = 0 \tag{6}$$

whose solution does not depend on the interface position between the ambient and dense fluids inside the porous medium. Solving Eq. (6) with boundary conditions Eqs. (1) and (3), the pressure field is obtained there. By considering a velocity potential $\phi = p - \rho g' z$, with $\nabla^2 \phi = 0$, the conjugate stream function ψ fulfills an equation similar to Eq. (6).

Note that the velocity potential ϕ and the stream function ψ inside the porous medium can only be found considering the boundary conditions independently of the time. This is because Eq. (6) is an elliptic differential equation or, from a physical point of view, the flow inside the porous medium adjusts to any upper boundary condition in a negligible time. Thus, it is not necessary to know the evolution of the gravity current front position at this stage of the analysis.

Fig. 7 shows the isolines of ϕ and ψ for different values of x_f/ε when the porous bed lies on an impermeable base. Solid lines centered at the front represent the streamlines that include 90 and 80% of the flow, while dashed lines are intermediate values. The 0.9 line starts about midway along the current ($x/x_f \sim 1/2$) in all cases. For $x_f/\varepsilon = 0.25$, the 0.9 line finishes at a rather far point involving a greater length of the upper boundary; however, the flow is always important just near the current front but not in the deeper part of the porous bed. The horizontal length of the zone with high flow increases slightly for $x_f > \varepsilon$, and the streamlines become almost semicircular for the greatest value of x_f/ε as shown in Fig. 7(d). In this case, the boundary conditions at $x = 0$ and $x_m \gg x_f$ do not strongly affect the flow because this is mainly confined to a horizontal length of the order of ε.

Fig. 8 shows the ϕ and ψ isolines obtained in the case of a porous bed with permeable lower boundary. Here the 0.9 line finishes at the lower boundary for all the depicted cases. In fact about 30% of the dense fluid flows through the lower boundary for $x_f/\varepsilon = 0.25$ [Fig. 8(a)], and this percentage increases for a decreasing thickness of the bed reaching 60% for $x_f/\varepsilon = 2$ [Fig. 8(d)]. The upper boundary for $x > x_f$ only participates significantly in the flow near $x/x_f \sim 1$, where the streamlines concentrate adopting a semicircular shape. The term ρg in Eq. (2) is not considered here for the sake of simplicity but it may become significant, as we will see below.

Thus, the flow between the upper boundaries at $x < x_f$ and $x > x_f$ of the porous layer dominates near the current front. It takes place between the surfaces at the same level and perpendicular to gravity, so that the mean pressure gradient in this zone may be estimated as

$$|\bar{\nabla} p| \approx \Delta p / \Delta x \tag{7}$$

where Δp is the pressure difference corresponding to a characteristic local horizontal length.

By using Eqs. (1) and (2) the order of magnitude of the flow per unit area is obtained

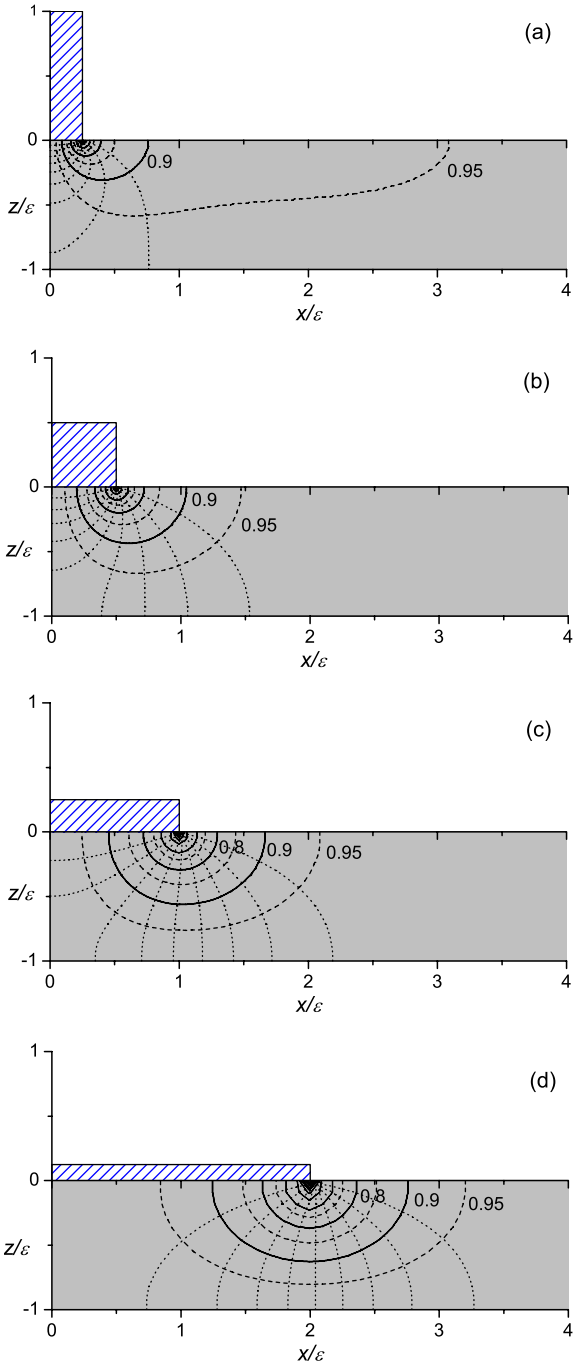

Fig. 7. Box model of gravity current (dashed region) spreading over porous medium (shadow region) with impermeable lower boundary, and lines with equal values of pressure p-$\rho g' z$ (dotted lines) and stream function ψ (solid and dashed lines) inside the bed: (a) $x_f/\varepsilon = 0.25$; (b) 0.5; (c) 1; (d) 2

$$q_f \approx \frac{\kappa}{\mu}\left(\frac{p_1}{\Delta x}\right) = \frac{\kappa}{\mu}\left(\frac{\rho_a g' h_f}{\Delta x}\right) \tag{8}$$

where h_f = local height that characterizes the gravity current leading part. Let us find now the vertical characteristic depth Δz for which the flow per unit transversal length Q_f is important. Thick and thin porous media is $\Delta z < x_f$ and $\Delta x \approx \varepsilon < x_f$, respectively. In any case we expect that $\Delta z \approx \Delta x$ and then

$$Q_f \approx q_f \Delta z = \frac{\kappa g'}{\nu} h_f \tag{9}$$

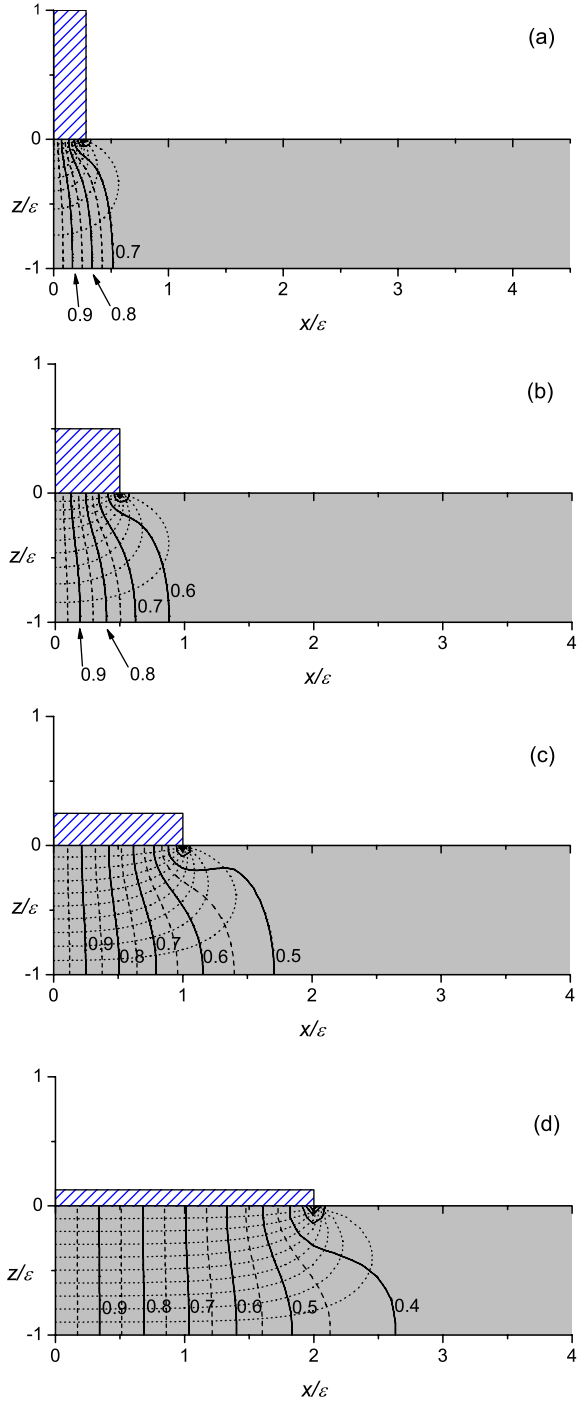

Fig. 8. Box model of gravity current of given volume spreading over porous medium with permeable lower boundary and lines with equal values of pressure p-$\rho g' z$ (dotted lines) and stream function ψ (solid and dashed lines) inside the bed: (a) $x_f/\varepsilon = 0.25$; (b) 0.5; (c) 1; (d) 2

where $\kappa g'/\nu$ = characteristic velocity of the flow through the porous medium known as "hydraulic conductivity" in the groundwater studies when $g' = g$. Thus, according to Eq. (9), the flow Q_f does not depend on the layer thickness.

The percolation through the porous medium from the upper boundary at the rear part of the current plays an important role in the case of extended currents and a permeable lower boundary, as seen in Fig. 8. In such a case, the term ρg in Eq. (2) may become significant and be taken into account using the model proposed by Thomas et al. (2004) as follow. As the gravity current travels significantly faster over the bed than the dense fluid penetrates into the porous layer, the dense fluid extends over a horizontal length much greater than the vertical depth η through which the current fluid percolates into the porous medium. In such a situation, the gravity current is approximated to a fluid layer of constant thickness $h \approx h_f$ and density ρ_c (box model), the pressure excess p_1 becomes uniform and the flow per unit area through the porous medium can be treated as one-dimensional. From Eq. (2) the vertical flow per unit area is

$$q_v = -\frac{\kappa}{\mu}\left(\frac{\partial p}{\partial z} + \rho g\right) \tag{10}$$

where the term ρg is kept without adding difficulty to this approximation.

The pressure gradient driving the fluid from the current into the bed is given not only by the difference in pressure excess p_1 at the top of the bed [see Eq. (1)] and the pressure $p(-\eta)$ at the interface located at $z = -\eta$ between the dense and ambient fluids, but also by the buoyancy of the dense fluid incorporated in the bed. Hence, Eq. (10) becomes

$$q_v = -\frac{\kappa}{\mu}\left(\frac{\rho_a g' h - p(-\eta)}{\eta} + \rho_a g'\right) \tag{11}$$

The vertical flow per unit area between the interface and the permeable bottom of the bed [where the pressure excess is $p = 0$, see Eq. (3)] is given by

$$q_3 = -\frac{\kappa}{\mu}\left(\frac{p(-\eta)}{\varepsilon - \eta}\right) \tag{12}$$

We assume that the length of the upper and lower boundaries of the bed involved in this flow is approximately the same. Continuity requires that $q_v \approx q_3$, and then

$$q_v = -\frac{\kappa}{\nu}\frac{g'(h+\eta)}{\varepsilon}. \tag{13}$$

The velocity of the interface per unit area, $\partial\eta/\partial t$, is related to q_v by means of the porosity φ of the porous layer by means of

$$\varphi\frac{\partial \eta}{\partial t} = q_v \tag{14}$$

and the volumetric flow per unit transversal length is

$$Q_v \approx q_v x_f \tag{15}$$

with

$$\frac{\kappa}{\nu}g'\frac{h_f}{\varepsilon}x_f < Q_v < \frac{\kappa}{\nu}g'\frac{(h_f+\varepsilon)}{\varepsilon}x_f \tag{16}$$

The ratio between the horizontal [Eq. (9)] and vertical [Eq. (15)] flows within the porous medium is

$$\frac{Q_f}{Q_v} \geq \frac{\varepsilon}{x_f} \tag{17}$$

Eq. (17) indicates when the vertical flow dominates and the one-dimensionality hypothesis used to reach Eq. (10) is valid. Otherwise, we can take Eq. (9) as an approximation of the flow that sinks into the permeable layer.

Evolution of Gravity Current

The gravity current evolves by changing the length x_f of the bed's upper boundary that is affected according to Eq. (1). Figs. 7 and 8 also illustrate the corresponding sequences of an idealized gravity

current of a homogeneous fluid. Its nonsteady evolution can be treated as a succession of steady states in which the pressure distribution inside the porous medium fulfills the boundary conditions Eq. (1) and (3) varying with time. It is assumed that the current slowly loses mass into the porous layer, which is a reasonable hypothesis for our experiments and a wide range of natural situations. Thus, the front velocity is

$$u_f = \mathsf{F}\sqrt{g' h_f}, \tag{18}$$

where $\mathsf{F} \sim 1$ is the Froude number (Marino et al. 2005 and references therein).

For the case of a permeable lower boundary of the porous medium, the flow into the bed near the front located between the upper boundaries $x < x_f$ and $x > x_f$ of the porous layer may only be important during the first part of the evolution of the current. As deduced from Eq. (17), this flow may be neglected for extended gravity currents. On the contrary, this is the main flow for the case of an impermeable lower boundary of the porous substrate. In such a case, mass conservation suggests that

$$Q_f = -\frac{dA}{dt} = -u_f \frac{dA}{dx_f} \tag{19}$$

where $A = h_f x_f$ = current lateral area or volume per unit length.

It is well known that gravity currents propagating on a rigid surface display phases described by particular features [see for instance Marino et al. (2005)]. In the first one, called "slumping" phase, the front velocity is constant and the current height at the front is of the order of $h_f \approx h_0/2$ (Simpson 1997). Therefore, for a gravity flow over a porous substrate, Eq. (19) allows us to find that the gravity current volume decreases linearly, that is

$$\frac{A}{A_0} \approx 1 - \alpha(x_f - x_0) \tag{20}$$

where

$$\alpha = \frac{\kappa}{\nu F x_0}\sqrt{\frac{2g'}{h_0}} \tag{21}$$

Eq. (20) implies that in this phase the dense fluid of the gravity current that seeps into the pores of the bed forms a layer of constant depth $\eta = \alpha A_0/\varphi$. Figs. 4 and 5 show that the theoretical approximation Eq. (20) reasonably agrees with the experimental findings, while Fig. 9 illustrates that experimental results satisfy Eq. (21).

Because our experimental setup does not allow us to measure for very long lengths of time (that is, for very extended currents), we may attempt to understand what happens analyzing the dynamics of gravity currents spreading on solid bottoms and adapting it to the present case. After the front advances a distance of about $10x_0$, the flow evolves to another regime in which velocity front decreases and a self-similar solution may be found from the shallow water equations. In this case, the front position as a function of time is

$$x_f = \xi(g'_0 A_0)^{1/3} t^{2/3} \tag{22}$$

where ξ = constant. Details of how this formula is found were reported by Marino et al. (2005) among others. Eq. (22) describes the asymptotic behavior for $t \gg t_c$, which is represented by dashed lines in Fig. 3. The front height is not constant in this stage and changes with x_f maintaining the current height profile shape that is given by

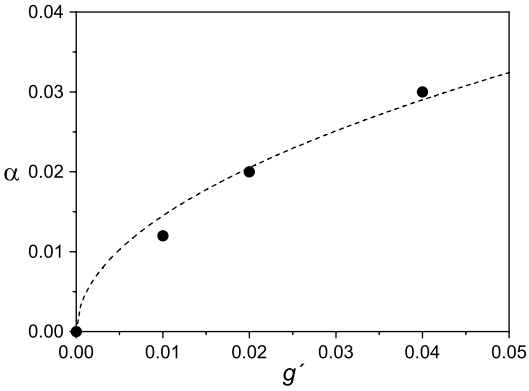

Fig. 9. Experimental data (symbols) of coefficient introduced in Eq. (20) as function of reduced gravity; relationship given by Eq. (21) is represented with dotted line

$$\frac{h(x/x_f)}{h_f} = \frac{x_f}{x}\left[\frac{\mathsf{F}^2}{4} + \left(1 - \frac{\mathsf{F}^2}{4}\right)\left(\frac{x}{x_f}\right)^2\right] \tag{23}$$

with

$$h_f = \frac{A_0}{I x_f} \tag{24}$$

where the shape factor [also used by Rottman and Simpson (1983) and Gratton and Vigo (1994)]

$$I = \int_0^1 (h/h_f)\cdot d(x/x_f) = \left(\frac{12}{12 - 2\mathsf{F}^2}\right) \approx 1.2 \tag{25}$$

does not depend on x_f.

If the mass is lost slowly into the porous bed, the flow over it can be treated as a succession of self-similar states in which the area A depends on time and

$$h_f = \frac{A(t)}{I x_f} \tag{26}$$

Under this hypothesis, the regime of the gravity current is quasi-self-similar, description which has been applied in other similar contexts (Gratton et al. 1996). Note that the relationship of Eq. (26) differs from that derived from the box model only by a factor I.

By solving the differential equation resulting from Eq. (19) and using Eqs. (9), (18), and (26) we obtain

$$\frac{A}{A_0} = \left\{1 - \left[\sqrt{\frac{x_f}{L}} - \sqrt{\frac{x_0}{L}}\right]\right\}^2 \tag{27}$$

where

$$L = \frac{A_0 \nu^2 \mathsf{F}^2 I}{\kappa^2 g'} = \frac{A_0}{\eta_c} \tag{28}$$

is a characteristic length that provides an approximated horizontal scale where the porous substrate affects the evolution of the gravity current, which is mainly related to a combination of the permeability, the reduced gravity, and the dense fluid viscosity. Note that we may also think L as a quotient of the initial volume per unit length, A_0, and the characteristic depth $\eta_c = \kappa^2 g'/I\nu^2\mathsf{F}^2$ of the interface between the dense and light fluids in the porous medium. Combining Eq. (28) with the characteristic front velocity of Eq. (18) at $t = 0$ we obtain the corresponding characteristic time

$$\tau = \frac{L}{u_f(t=0)} = \frac{A_0 \nu^2 \mathsf{F}}{\kappa\sqrt{h_0 g'^3}} \tag{29}$$

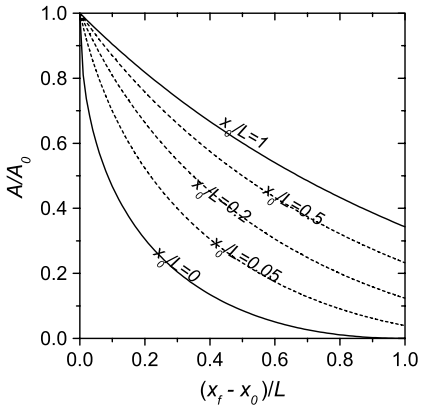

Fig. 10. Dimensionless gravity current lateral area as function of characteristic lengths ratio

Another interesting observation associated with Eq. (27) is that concerning to the ratio x_0/L. Fig. 10 shows that the smaller this ratio is, the higher the loss of dense fluid into the porous substrate in the same distance run by the front. The fast drop of the transversal area displayed by the gravity current for $x_0 \ll L$ is because of the high value of h_f involved for the same A_0 in the initial moments of spreading.

Final Remarks

The influence of an impermeable surface below a porous bed on the evolution of plane inertial gravity currents mass was investigated experimentally varying the volume of the dense fluid released, the relative difference of density, and the thickness of the bed extending the case studied by Thomas et al. (2004).

The developed analytical treatment provides a physical insight of the main fluxes over and through the porous medium. The experiments performed, in which the bed is modeled using small glass spheres, show new interesting aspects such as the effects of the roughness of the medium's upper boundary on the current dynamics that may be related to erosive-sedimentary processes in natural situations. The current decelerates as the driving pressure decreases because of the current thinning because of the sinking of fluid into the bed, but significant changes in the evolution of the front position or its velocity take place outside the maximum extension of our experimental setup. We describe the flow dynamics in terms of a quasi-steady-state global mass balance, suggesting analytical approximations, and find that the flow of ambient fluid from the bed ahead of the current front may be significant, particularly if the depth of the layer is greater than the extension of the current [see Eq. (17)]. The expressions that allow estimating the depth of dense fluid layer inside the porous bed are given while, as opposed to that obtained by Thomas et al. (2004), no exponential decreasing of the current mass is determined for the case of a porous bed with an impermeable lower boundary.

The measurements of the mass do not show a clear dependence of h_0 and x_0 separately in agreement with Eqs. (27) and (28). The situation resembles others where gravity flows evolution does not strongly depend on the height profile, mixing, Froude number at the front, details of the fluid's release, and the initial fractional depth of the dense fluid. Therefore, the behavior of the flows involved seems to be insensitive to these variables. Instead, the decreasing of the mass is associated with the characteristic lengths L or $1/\alpha$ given by Eqs. (28) and (21), respectively, which makes M a good experimental parameter to validate analytical relationships and complex numerical codes.

Acknowledgments

Financial support for this study was provided by ANPCyT (PICT 1185/06) and CONICET (PIP 0054/10), Argentina.

Notation

The following symbols are used in this paper:

A = current lateral area of the gravity current;
F = Froude number at current head;
g' = initial reduced gravity;
h = current height;
I = shape factor;
L = characteristic length;
M = dimensionless gravity current mass;
m = current mass per unit width;
p = pressure;
Q_f = flow per unit transversal length within porous bed;
q = flow per unit area within porous bed;
q_v = vertical flow per unit area within porous bed;
q_3 = vertical flow per unit area between interface and permeable bottom of bed;
R = Reynolds number of current;
R_{PM} = Reynolds number of the flow through porous medium;
t = time;
t_c = characteristic time of gravity current;
u = current velocity;
v = vertical component of velocity of dense fluid inside porous bed;
x = horizontal position of current front;
z = vertical coordinate;
α = coefficient in the law of mass evolution;
β, ξ = constants;
ε = thickness of porous bed;
η = depth of dense fluid inside porous bed;
η_c = characteristic depth of dense fluid inside porous bed;
κ = permeability of bed;
μ = dynamic viscosity;
ν = kinematic viscosity;
ρ_a, ρ_c = density of ambient fluid and current fluid;
τ = characteristic time of flow within porous bed;
τ_D = constant of decay for viscous flow through porous medium;
τ_I = constant of decay for inertial flow through porous medium;
ϕ = velocity potential;
φ = porosity of bed; and
ψ = conjugate stream function of velocity potential.

Subscripts

0 = initial values; and
f = values at the front.

References

Acton, J. M., Huppert, H. E., and Worster, M. G. (2001). "Two-dimensional viscous gravity currents flowing over a deep porous medium." *J. Fluid Mech.*, 440, 359–380.

Bear, J. (1972). *Dynamics of fluids in porous media*, Elsevier, New York.

Dalziel, S. B. (2006). *DigiFlow User Guide*, ⟨http://www.dalzielresearch.com/digiflow/⟩ (Jan. 20, 2012).

Gratton, J., and Vigo, C. (1994). "Self-similar gravity currents with variable inflow revisited: Plane currents." *J. Fluid Mech.*, 258, 77–104.

Gratton, R., Diez, J. A., Thomas, L. P., Marino, B. M., and Betelu, S. (1996). "Quasi-self-similarity for wetting drops." *Phys. Rev. E*, 53(4), 3563–3572.

Haber, S., and Mauri, R. (1983). "Boundary conditions for Darcy's flow through porous media." *Int J. Multiphas Flow*, 9(5), 561–574.
Hacker, J., Linden, P. F., and Dalziel, S. B. (1996). "Mixing in lock-release gravity currents." *Dyn. Atmos. Oceans*, 24(1–4), 183–195.
Marino, B. M., and Thomas, L. P. (2002). "The spreading of a gravity current over a permeable surface." *J. Hydraul. Eng.*, 128(5), 527–533.
Marino, B. M., and Thomas, L. P. (2010). "Gravity flows associated with erosive-sedimentary processes in rivers and estuaries beds." *Proc. Latin American Congress on Hydraulics*, IAHR, Punta del Este, Uruguay, 1A_335.
Marino, B. M., Thomas, L. P., and Linden, P. F. (2005). "The front condition for gravity currents." *J. Fluid Mech.*, 536, 49–78.
Moodie, T. B., and Pascal, J. P. (1999a). "Axisymmetric spreading and filtration of inclined thermals over porous surfaces." *Can. Appl. Math. Q.*, 7(2), 185–201.
Moodie, T. B., and Pascal, J. P. (1999b). "Downslope movement of compositionally driven gravity currents over porous surfaces." *J. Porous Media*, 2(2), 127–141.
Prinos, P., Sofialidis, D., and Keramaris, E. (2003). "Turbulent flow over and within a porous bed." *J. Hydraul. Eng.*, 129(9), 720–733.
Pritchard, D., and Hogg, A. J. (2002). "Draining viscous gravity currents in a vertical fracture." *J. Fluid Mech.*, 459, 207–216.
Pritchard, D., Woods, A. W., and Hogg, A. J. (2001). "On the slow draining of a gravity current moving through a layered permeable medium." *J. Fluid Mech.*, 444, 23–47.
Rottman, J. W., and Simpson, J. E. (1983). "Gravity currents produced by instantaneous releases of a heavy fluid in a rectangular channel." *J. Fluid Mech.*, 135, 95–110.
Simpson, J. E. (1997). *Gravity currents in the environment and the laboratory*, Cambridge University Press, Cambridge, U.K.
Spannuth, M. J., Neufeld, J. A., Wettlaufer, J. S., and Worster, M. G. (2009). "Axisymmetric viscous gravity currents flowing over a porous medium." *J. Fluid Mech.*, 622, 135–144.
Thomas, L. P., Dalziel, S. B., and Marino, B. M. (2003). "The structure of the head of an inertial gravity current determined by particle tracking velocimetry." *Exp. Fluids*, 34(6), 708–716.
Thomas, L. P., Marino, B. M., and Linden, P. F. (1998). "Gravity currents over porous substrates." *J. Fluid Mech.*, 366, 239–258.
Thomas, L. P., Marino, B. M., and Linden, P. F. (2004). "Lock-release inertial gravity currents over a thick porous layer." *J. Fluid Mech.*, 503, 299–319.
Ungarish, M., and Huppert, H. E. (2000). "High-Reynolds number gravity currents over a porous boundary: Shallow-water solutions and box-model approximations." *J. Fluid Mech.*, 418, 1–23.